DEPARTMENT OF THE INTERIOR

U. S. GEOLOGICAL SURVEY

Time-to-Failure Analysis of Seismicity Preceding the 1989 Loma Prieta Earthquake

by

Charles G. Bufe[1] and David J. Varnes[1]

Open-File Report 90-666

This report is preliminary and has not been reviewed for conformity with U. S. Geological Survey editorial standards.

[1] U. S. Geological Survey, Golden, Colorado

1990

Abstract. Seismicity in northern California shows a long-term regional pattern of accelerating seismic-energy release leading up to the October 18, 1989 Loma Prieta earthquake. This pattern is apparent in cumulative sums of both seismic moment and square root of energy or moment. More than a year before the Loma Prieta earthquake, the integrated form of the INPORT relation (Varnes, 1989) was applied to cumulative sum of square root of energy, which was estimated from magnitude: this analysis indicated a failure time of 1996. Post-earthquake refinements to this time-to-failure analysis of seismicity, utilizing seismic-moment release, Benioff strain-energy release, and event counts, indicate that a large earthquake (Loma Prieta) in the southern San Francisco Bay region could have been anticipated to occur within a year or two after June, 1989. Simulations of the evolution of time-to-failure forecasts for the 1906 San Francisco and 1989 Loma Prieta earthquakes illustrate the potential usefulness and limitations of such forecasts. The error in the forecast generally decreases as the time of the mainshock approaches. The inversion for time of failure for the Loma Prieta earthquake can be stabilized by constraining the exponent of time to failure on the basis of foreshock (and aftershock) data for other main shocks from the same region (i. e., 1906) or on the basis of b-value (slope of log frequency of occurrence as a function of magnitude) for the data set. Uncertainties surrounding the selection of the time window for analysis can be overcome by superposing accelerating (foreshock) and decelerating (1906 aftershock) sequences. The "postdiction" of the prior occurrence of the 1836-1838 earthquakes through analysis of the decelerating 1855-1890 seismicity indicates these analysis techniques may also have the potential to provide, for some regions, useful information on the occurrence of large earthquakes predating the historical record.

Introduction

Varnes (1983) has shown that creep curves for various materials show decelerating (primary) and accelerating (tertiary) creep; these processes may proceed concurrently as well as in succession. The most common form of accelerating creep is characterized by the INPORT relation, i.e. the *rate* is proportional to the INverse Power Of Remaining Time to failure. Varnes (1989) has shown that Benioff strain energy release in foreshocks often follows this relation, and when it does, the time of the main shock may be predicted from the pattern of accelerating energy release.

Epicenters of earthquakes of magnitude 5 and larger in northern California are shown in Figure 1 for the period 1836 through 1989. In this paper we analyze seismicity in the union of three rectangular regions (northern, central, and southern, or N,C,S in Figure 1). This composite region, which was selected for analysis in 1988 (prior to the occurrence of the Loma Prieta earthquake), includes the San Andreas and subsidiary fault systems opposite the rupture zone of the 1906 earthquake, and is bounded on the south by the beginning of the creeping section of the San Andreas fault and on the west, north, and east by relatively aseismic regions. We also analyze seismicity in the smaller central (C) and southern (S) zones, the latter defined to include the aftershock zone of the M_S 7.1 Loma Prieta earthquake. Long-term seismicity patterns prior to the 1906 and 1989 earthquakes show accelerating rates of energy release. This is shown in Figure 2 (for M_L 5 and larger), where the cumulative moment, square root of energy (both computed from magnitudes), and event count for the combined regions (N,C,S) are plotted as a function of time, beginning in 1855. In Figure 3 the pre-step values (the plus symbols in Figure 2) of cumulative seismic moment and cumulative Benioff strain-energy release are plotted for the period 1927 to 1988. We also analyzed post-step and mid-step values, but found that the pre-step data provide more consistent and accurate estimates of t_f. When pre-step values are used, the increment associated with a given earthquake is plotted at the time of the following event. This is analogous to use of the lower bounds of cumulative moment in the precise recurrence (time-predictable) model of Bufe, Harsh, and Burford (1977).

The increase in seismicity seen in Figure 3 was noted as early as the 1950's by Tocher (1959) and has been discussed by Ellsworth and others (1981). The pattern was interrupted by a period of relative quiescence in the 1960's and 1970's (extending to all of California and surrounding regions) which ended (Bufe and Toppozada, 1981) in northern California in 1979 with the occurrence of the Coyote Lake earthquake.

This paper develops techniques for forecasting large earthquakes with an accuracy of a few years using the long-term acceleration in regional seismicity that sometimes precedes events like the 1989 Loma Prieta, the 1906 San Francisco, and the 1868 Hayward earthquakes. Testing these techniques on data sequences preceding other earthquakes will be the topic of another paper.

Data Analysis

Varnes (1989) has shown that a number of foreshock sequences follow a relation of the form:

$$d\Sigma E^{0.5}/dt = k/(t_f-t)^n, \qquad (1)$$

which we will refer to as the INPORT (INverse Power Of Remaining Time) relation. Integrated, this becomes:

$$\Sigma E^{0.5} = \Delta + (k/(n-1))(t_f-t)^m, \qquad (2)$$

where E is strain energy calculated from magnitude, Δ, k, and n are constants, m=1-n, $n \neq 1$, and t_f is time of failure (main shock).

The above equations can be generalized to apply to various earthquake parameters (EQP's, or Ω's), such as seismic moment, or event count, as well as square root of energy (or of moment). The Ω is usually estimated from earthquake magnitude by an equation of the form:

$$\log \Omega = cM + d. \qquad (3)$$

The coefficient c equals 1.5 for moment or energy, 0.75 for square root of moment or energy, and zero for event count.

The INPORT relation is equivalent to the modified Saito relation used to describe tertiary creep (Varnes, 1983). Differentiation of (1) results in the equation:

$$d^2\Omega/dt^2 = nk/(t_f-t)^{(n+1)} = nk^{1-(n+1)/n} (d\Omega/dt)^{(n+1)/n}. \qquad (4)$$

Letting $\alpha = (n+1)/n$, and $A = nk^{-1/n}$, we have:

$$d^2\Omega/dt^2 - A (d\Omega/dt)^{\alpha} = 0. \qquad (5)$$

This is equation (20) of Voight (1989), who reports rate-dependent material failure processes with α values between 1 and 3, with a preference for $\alpha=2$.

The time-to-failure technique, which has application to both short-term (Varnes, 1989) and intermediate-term (this paper) earthquake forecasting, was applied to seismicity in the union of the three rectangular regions in northern California shown in Figure 1. The southern region (S) is approximately centered on the Loma Prieta earthquake and contains the 1984 Morgan Hill earthquake (M_L 6.2) near its northern edge. The central region (C) contains the rupture zones of the two large Hayward fault earthquakes of 1836 and 1868. The large 1838 earthquake on the San Francisco peninsula is contained in regions S and C. The northern region (N) contains only four earthquake epicenters that are separated from the central region by a 60-km gap. The union of these regions corresponds roughly to the San Andreas fault system (this includes

the Calaveras, Hayward, and other related faults) opposite the 1906 rupture zone. Varnes' unpublished original analysis of seismicity in this region was done more than one year prior to the October 18, 1989, Loma Prieta earthquake. Cumulative strain energy release ($\Sigma E^{0.5}$) was calculated from magnitudes tabulated by Ellsworth and others (1981) for events through 1980. For most events, these magnitudes are consistent with the Berkeley M_L magnitudes. Berkeley magnitudes (M_L) were used for more recent earthquakes. A best fit regression analysis for equation (2) was made using all events of magnitude 5 and larger from 1927 through June of 1988; both t_f and m were allowed to vary. The 1927 event was followed by 12 years of quiescence, providing a baseline for the later acceleration in Ω. Varnes' analysis, which was done on a pocket programmable calculator and lacked resolution in t_f, indicated a time of failure of 1996. Thus a large earthquake was to be expected in northern California within a few years. The occurrence, on October 18, 1989, of the Loma Prieta earthquake demonstrated the utility of the time-to-failure technique and provided the impetus for a more detailed analysis of the data.

Further computer analysis, after the Loma Prieta earthquake, of these same data used the Nelder-Meade simplex nonlinear least squares algorithm (Dennis and Woods, 1987) to invert for t_f and m. The best fit (curve in Figure 3(b) and first row of Table 1) to 1927.1-1988.5 cumulative square root of energy data occurs when m is 0.35 and t_f is 1990.0. This date is within three months of the time of the Loma Prieta earthquake. A non-dimensional measure of goodness of fit to these data (rms error derived from the least squares inversion algorithm divided by range of data) is contoured in Figure 4 as a function of t_f and exponent m. An elongated, asymmetric minimum or zone of best fit is seen, with the location of minimum error indicated by the large dot. The small dot shows Varnes' original (1988) estimate.

For positive m, the technique also provides an estimate of the magnitude of the expected event at t_f. This is because the rate $d\Omega/dt$ is infinite at t_f, but the computed value of Ω is not. Thus we have a finite value of Ω at t_f from which we can predict a magnitude. For the pre- Loma Prieta earthquake data analysis shown in Figure 3(b), this predicted magnitude is 6.83. Magnitude computed for the Loma Prieta earthquake range from an M_L of 6.7 based on strong motion records (Uhrhammer and Bolt, 1990) to the teleseismically-determined USGS M_S of 7.1. The predicted magnitude is close to the Loma Prieta moment magnitude of 6.9 (Kanamori and Helmberger, 1990). For the great 1906 San Francisco earthquake, fixing m at 0.35 and inverting the data set that includes magnitude 5.5 and larger pre-1906 earthquakes (from 1855 to 1903) provides a time of failure of 1906.2 and a magnitude estimate of 7.64. The moment magnitude of the 1906 earthquake has been estimated at 7.7 (Hanks and Kanamori, 1979).

The analysis of the pre- Loma Prieta data was repeated for various time periods and magnitude cutoffs and for seismic moment and event count as well as for square root of energy data. The results are shown in Table 1. Equivalent exponents m, n, and α, in equations (2), (1), and (5) respectively, are tabulated. The top half of Table 1 displays the results of unconstrained (m, t_f free) attempts to fit the data. Few analyses of the cumulative event count (N) data sets converge to yield a time of failure (t_f). The estimates of t_f based on seismic moment data are consistently late. Estimates based on Benioff strain energy release ($E^{0.5}$) data generally fall within a year of the time of the Loma Prieta earthquake (1989.8). The analysis of Benioff strain energy release data from 1927.1 to 1989.6 (magnitude 5 and above) for the southern (S) region provides an excellent estimate of time (1989.9) for the Loma Prieta earthquake, but underestimates its magnitude as 6.3. This suggests that events within about 70 km of the Loma Prieta epicenter are sufficient to predict time of occurrence, but that the premonitory increase in seismicity for the magnitude 7 Loma Prieta earthquake extends outward to a somewhat greater distance.

For pre-1906 earthquake data, the catalog appears to be incomplete below magnitude 5.5. Free determinations of m and t_f for pre-1906 data (magnitude 5.5 and larger) are given in Table 1. In general, fits to data preceding the 1906 earthquake do not converge unless m or t_f

are fixed. Free solution for t_f and m from the acceleration preceding the M_L 6.7 Hayward fault earthquake of October 21, 1868, however, predicts a mainshock of about magnitude 7 in 1866 or 1867.

The first few rows of Table 1 indicate that the results for m and t_f depend on the time window used in the analysis. Because it may not be obvious when the long-term aftershocks of a previous large event end and the long-term foreshocks of the next large event begin, the selection of a time window is somewhat arbitrary. In order to address this problem, we have analyzed in Figure 5 cumulative seismic moment data for magnitude 5.5 and larger events for the entire period between the 1906 San Francisco and the 1989 Loma Prieta earthquakes. The data were fitted by superposition of two equations in the general form of equation (2) with the same exponent; one equation describes deceleration of moment rate following the past large event (aftershocks) and the other describes acceleration of moment rate preceding the future large event (foreshocks). This is analogous to the superposition of primary and tertiary creep processes in earth materials described by Varnes (1983). The predicted time of failure (see Table 1, third row from bottom) is late by two years or more. One possible reason for this is that aftershocks, while usually obeying Omori's Law, may be characterized by exponents different from those for foreshocks. Another reason for different exponents may be that the Loma Prieta earthquake is not a recurrence of the 1906 earthquake but an integral part of the long-term buildup to the next major earthquake (as the M_L 6.7 Hayward fault earthquake of 1868 appears to be part of the overall buildup preceding 1906). The exponent of time to (or from) failure may not be scale invariant for a given region, although the results presented below suggest that it is for large earthquakes in northern California.

For some of the data sets in Table 1, there is no stable solution for m and t_f. While it is often possible to determine "best fit" values for both t_f and m from the data, in other cases the exponent m may be unstable in the free solution. Two approaches for independently estimating m are presented here.

1. The exponent m is determined from seismicity preceding a previous large earthquake from the same region. This was done for the Loma Prieta earthquake using the data preceding the 1906 San Francisco earthquake to determine m (see Table 1, rows 11 and 12). Values of m determined for the periods 1856-1903 and 1870-1903 (eliminating the buildup before the Hayward fault earthquake of 1868) were averaged and used in analysis of the pre- Loma Prieta data. This procedure accurately predicts the time of failure for the Loma Prieta earthquake using the seismic moment data for either the southern (Table 1, row 14) or the combined (row 13) data sets. The results for Benioff strain-energy release are nearly as good. It is also interesting to note that moment, strain-energy release, and event count data through 1980 (Table 1, row 15) all indicate a 1985 time of failure for the central (C) zone. This zone is closer to the M_L 6.2 Morgan Hill earthquake of April 24, 1984, than to the Loma Prieta event. Seismicity in the central zone may have been influenced by processes culminating in the Morgan Hill earthquake, as no magnitude 5 or larger events occurred in this zone after 1980.

2. For a model of regularly occurring events of increasing magnitude, following the INPORT relation, Varnes (1989) has shown that the product nb is a constant, where n=1-m and b is from the relation

$$\log N = a - bM \qquad (6)$$

where M is magnitude and N is number of earthquakes of magnitude M or greater. For this simple model, it can be shown that this constant is the coefficient c in equation (3). Thus:

$$m = (b-c)/b. \qquad (7)$$

Using this approximation, m will be negative when Ω is seismic moment or energy (c = 1.5). However, m will be positive for most data sets (b > 0.75) when Ω is square root of energy or of moment (c = 0.75). The b parameter can be computed for the earthquake data set used to

estimate t_f. The b value for magnitude 5 and greater earthquakes from 1927.1 to 1989.6 in the combined regions (N,C,S) is 1.23. Using equation (7), this b value translates to m values of .391 for Benioff strain-energy release and -0.220 for seismic moment. Figure 6 shows a measure of goodness of fit to the data (rms residual divided by range of data) contoured as a function of the coefficient c (by which Ω is defined) and the exponent m (which determines the acceleration of the cumulative Ω as we approach t_f). In order to explore the relations among c, m, and goodness of fit, we fix t_f at the time of the Loma Prieta earthquake. Relatively low residuals extend from (c=0, m=.75) to (c=1.5, m=-.15), with the minimum occurring near (c=.75, m=.35). This minimum indicates a better fit for Benioff strain-energy release data than for event count or seismic moment release data. Equation (7), with b=1.22, is shown as the dashed line on Figure 6.

Model-based analyses for data sets for the combined zones and for the southern zone alone for the period 1927.1-1989.6 are tabulated at the bottom of Table 1. Exponent values are calculated for the estimated b value and for its 95% confidence limits. The t_f's for Loma Prieta are on target using the Benioff strain-energy release data, but about two years late using seismic moment data.

From equation (7), if m=1 then c=0 for all b, and the rate of occurrence of events is constant with time. An extreme model representing an opposite end member would attribute the acceleration in Ω of a precursory series entirely to the occurrence of an increasing number of events of constant magnitude. For such a model, b is infinite, and m does not depend on b as in equation (7).

Fixing the value of exponent m decreases the scatter in solutions for t_f and magnitude for partial data sets and allows us to simulate the evolution of an earthquake forecast with time as data accrue. Such simulations are shown for the Loma Prieta earthquake in Figure 7 and for the 1906 San Francisco earthquake in Figure 8.

It is readily seen from examination of Figure 7 that early in the data set, when the acceleration curve is poorly defined, there would have been a high potential for false alarms for earthquakes of about magnitude 6. We have found from other analyses that the false alarm rate is lower when exponent m is not fixed, because the inversion for t_f will fail to converge for many of the data sets. From Figure 7, forecasts of a magnitude 7 or larger earthquake (Loma Prieta?) could have begun in 1969. The estimated time of failure for this event would have been updated with the occurrence of each new earthquake of magnitude 5 or larger. This update would have occurred, in each case, before the date of the previously estimated time of failure. By 1979, the forecast time of failure would have advanced to 2008 and the magnitude escalated to 7.6. The accelerating energy release between 1979 and 1989 would have led to convergence on the time (1989.8) and magnitude (6.9 to 7.1) of the Loma Prieta earthquake, with five consecutive stable, accurate ($\pm$ 1.5 years) forecasts during 1986-1989.

The computations of time of failure and expected magnitude for the pre-1906 data, shown in Figure 8, demonstrate an interesting feature of our analysis technique. The initial few years of data show a deceleration of energy release with time. The analysis program interprets these as aftershocks of an unspecified earlier event and tries to determine the occurrence time and magnitude of this previous main shock. The resulting "postdicted" main shocks therefore fall below the diagonal dotted line in Figure 8b. After 1865, a short term forecast existed for an earthquake in the magnitude 6 to 7 range, perhaps in anticipation of the 1868 magnitude 6.7 earthquake (indicated by the horizontal dashed line) on the Hayward fault. Following a decade of quiescence at the magnitude 5 level, the analysis resumes in the 1880's. The cumulative strain energy release data from 1855 to the 1880's show deceleration and the analyses converge sharply in time on the late 1830's. It appears that the data reflect the occurrence of the 1838 magnitude 7+ earthquake on the San Andreas fault and possibly the 1836 magnitude 6.8 earthquake on the Hayward fault (see Figure 8b). The 1838 earthquake is the largest historically recorded earthquake before 1906 and was believed by Louderback (1947) to be comparable in size to the 1906 earthquake. It is interesting that the analysis "postdicts" the

occurrence of this event and estimates its magnitude to be comparable to that of the 1906 earthquake (dashed line in Figure 8a).

Subsequent data show a transition from deceleration to acceleration in 1892 and show consistent forecasts (Figure 8a) of time of failure (1906 ±5 years) could be made from 1893 to the last pre-1906 data point in 1903. The forecasted magnitude (Figure 8a) ranges from 7.6 to 8.1.

Results and Discussion

The results shown in Table 1 demonstrate the consistency of estimates of time of failure, t_f, for the 1989 Loma Prieta and 1906 San Francisco earthquakes, using different data sets and different methods of estimating the exponent in the INPORT relation. The inherent uncertainty or scatter in the estimates is on the order of plus or minus 2 years. For these data, best results seem to be obtained using square root of energy as Ω. Use of this parameter also permits estimates of the magnitude of the forecast event because, for this data set, $\Sigma\Omega$ is finite at t_f. However, the use of square root of energy as Ω is theoretically undesirable because, for $b > 0.75$, the contribution to $\Sigma\Omega$ per magnitude unit increases as magnitude decreases. If relation (6) holds for very low magnitudes, $\Sigma\Omega$ over all magnitudes is unbounded. However, the events used in our time-to-failure analyses span two magnitude units or less. The values determined for m and t_f do not appear to be strongly dependent on the minimum magnitude used in the analysis (see Table 1, columns 7-10). As a rule of thumb, the minimum magnitude considered should be about two magnitude units below the magnitude of the event being forecast. This implies that a data set of 100 or fewer events is adequate. Analyses using event counts are much more likely to be affected by changes in minimum magnitude. Use of seismic moment or energy is generally not subject to this problem because c>b in almost all cases. However, we believe that examination of a range of Ω's, including event count ($c = 0$), square root of energy ($c = 0.75$), moment ($c = 1.5$), and magnitude ($c = 1$) may be useful in an empirical approach to earthquake forecasting.

Refinements in the time-to-failure method of earthquake forecasting are no doubt possible, and will result from improved understanding of the physical processes involved and from empirical studies of seismicity preceding large earthquakes. Varnes (1989) has shown, through analysis of data from a number of traditional (relatively short-term) foreshock sequences, that it may be possible to predict time of failure with a median error of about 30% of remaining time. By analogy, time-to-failure analyses of regional seismicity over periods comprising a significant fraction of the recurrence times for large characteristic (or uncharacteristic) earthquakes may provide a useful, improved estimate of the regional state of stress and of where we are in the seismic cycle. While the physical processes leading to the observed long-term acceleration in regional seismic-energy release are not well understood, they are probably related to either an accelerating regional strain rate at depth or, as suggested by Jones and Molnar (1979), to the progressive failure of asperities and concentration of stress on the remaining locked zones

Keilis-Borok and Kossobokov (1986, 1988) have systematically applied pattern-recognition algorithms to seismicity in large regions of the western U. S. and elsewhere around the world. Their prediction of a large earthquake in the California-Nevada region was evaluated by the U. S. National Earthquake Prediction Council (Updike, 1989). They also anticipated magnitude 7 earthquakes within two large (500 km diameter) circular zones which overlap in the vicinity of the Loma Prieta earthquake (see Figure 1). Sykes and Jaume' (1990) have also examined temporal variation in release of seismic moment for northern California. Like us, they have concluded that the zone of accelerating seismicity encompasses a region extending beyond the segment along the San Andreas fault which ruptured in the Loma Prieta earthquake.

Conclusions

The Morgan Hill and Loma Prieta earthquakes appear to satisfy, by virtue of the expected magnitudes and occurrence times, the patterns of accelerating energy release calculated from seismicity in the central (C) zone, the southern (S) zone, and the combined (N,C,S) zones. However, because the increased seismicity was observed for a large region encompassing both the San Andreas and Calaveras fault systems, and because the resolution of the time-to-failure determination may have an uncertainty of a few years, it is difficult to rule out the occurrence of additional earthquakes of comparable magnitudes on these systems in the next year or two. It is also likely that the Morgan Hill and Loma Prieta earthquakes are part of a longer-term buildup to a recurrence of the 1906 San Francisco earthquake or to a large earthquake anticipated for the San Francisco Bay area in the next several decades (Working Group on California Earthquake Probabilities, 1990).

Independent determination of the exponent of time to failure from other model parameters (such as b-value) or from foreshocks or aftershocks of previous large events appears to improve the determination of t_f for most of the pre- Loma Prieta data sets. Although the buildup of seismicity preceding the 1906 earthquake has a longer duration and is followed by a period of relative quiesence before the main shock, this data set provides a basis for independently determining the exponent in the INPORT relation used to analyze the data from the period preceding the Loma Prieta earthquake. Simulation of time-to-failure forecasts of large earthquakes, using the 1906 San Francisco and 1989 Loma Prieta earthquakes as examples, indicates the usefulness of this approach. However, the accelerating cumulative energy-release curves must span a long enough period and be sufficiently developed to define time of failure. Premature applications of these techniques on inadequate data bases have a high potential for false alarms, especially when a solution for time of failure can only be found by fixing the exponent m. Simulation of part of the seismic cycle by superposition of long term decelerating (1906 aftershock) and accelerating (Loma Prieta foreshock) sequences provides a means of describing seismicity since 1906. This approach eliminates the need to estimate when the inflection point occurs and when to begin the data set for the accelerating sequence.

The time-to-failure technique has application to both short-term (Varnes,1989) and intermediate-term earthquake forecasting (this paper). By examining long-term foreshock and aftershock sequences, these analysis techniques can provide useful information on both future and past failure processes. This approach is being evaluated on other earthquake data sets around the world as a tool to test and refine estimates of seismic potential such as those developed by Nishenko (1989) and Keilis-Borok and Kossobokov (1986, 1988).

References

Bufe, C. G., Harsh, P. W., and Burford, R. O., 1977, Steady state seismic slip - a precise recurrence model: Geophys. Res. Lett., v. 4, p. 91-94.

Bufe, C. G., and Toppozada, T. R., 1981, California earthquakes: end to seismic quiesence: California Geology, v. 34, p. 111-114.

Bufe, C. G., and Varnes, D. J., 1990, Accelerating seismic energy release preceding the 1989 Loma Prieta, California earthquake: EOS Trans. AGU, v. 71, p. 553.

Dennis, J. E., Jr., and Woods, D. J., 1987, New computing environments: microcomputers in large-scale computing, Wouk, A., editor, SIAM, p. 116-122.

Ellsworth, W. L., Lindh, A. G., Prescott, W. H., and Herd, D. G., 1981, The 1906 San Francisco earthquake and the seismic cycle: in Simpson, D. W. and Richards, P. G., eds., Earthquake Prediction: An International Review, Maurice Ewing Ser., v. 4, p 126-140, AGU, Washington, D.C.

Hanks, T. H., and Kanamori, H., 1979, A moment magnitude scale: J. Geophys. Res., v. 84, p. 2348-2350.

Jones, L. M., and Molnar, P., 1979, Some characteristics of foreshocks and their possible relationship to earthquake prediction and premonitory slip on faults: J. Geophys. Res., v. 84, p. 3596-3608.

Kanamori, H., 1977, The energy release in great earthquakes: J. Geophys. Res., v. 82, p. 2981-2987.

Kanamori, H., and Helmberger, D. V., 1990, Semi-realtime study of the Loma Prieta earthquake using teleseismic and regional data: EOS Trans. AGU, v. 71, p. 291.

Keilis-Borok, V. I., and Kossobokov, V. G., 1986, Time of increased probability for the strongest earthquakes of the world (in Russian): Comput. Seismol., v. 19, p. 48-57.

Keilis-Borok, V. I., and Kossobokov, V. G., 1988, Premonitory activation of seismic flow: Algorithm M8: Workshop, Global Geophysical Informatics with Applications to Research in Earthquake Predictions and Reduction of Seismic Risk, International Centre for Theoretical Physics, Trieste, Italy, H4.SMR/303-10.

Louderback, G. D., 1947, Central California earthquakes of the 1830's: Bull. Seism. Soc. Am., v. 37, p. 33-74.

Nishenko, S. P., 1989, Circum-Pacific seismic potential 1989-1999: U. S. Geological Survey Open-File Report 89-86, 126 pp.

Sykes, L. R., and Jaume', S. C., 1990, Seismic activity on neighboring faults as a long-term precursor to large earthquakes in the San Francisco Bay area: Nature, v. 348, p. 595-599.

Tocher, Don, 1959, Seismic history of the San Francisco region: California Division of Mines Special Report 57, p. 39-48.

Uhrhammer, R. A., and Bolt, B. A., 1990, Comparison between near and far-field estimates of the magnitude, energy, and moment of the Loma Prieta mainshock: EOS Trans. AGU, v. 71, p. 1455.

Updike, R. G., 1989, Proceedings of the National Earthquake Prediction Evaluation Council, June 6-7, 1988, Reston, Virginia: U. S. Geological Survey Open-File Report 89-144.

Varnes, D. J., 1983, Time-deformation relations in creep to failure of earth materials: Proc. 7th Southeast Asian Geotechnical Conf., v. 2, p. 107-130.

Varnes, D. J., 1989, Predicting earthquakes by analyzing accelerating precursory seismic activity: PAGEOPH, v. 4, p. 661-686.

Voight, B., 1989, A relation to describe rate-dependent material failure: Science, v. 243, p. 200-203.

Working Group on California Earthquake Probabilities, 1990, Probabilities of large earthquakes in the San Francisco Bay region, California: U. S. Geological Survey Circular 1053, 51 pp.

Table 1. Exponents (m, n, or α) and time of failure (t_f) determined by curve fitting to cumulative earthquake parameter (Ω) data. Mmin is the minimum magnitude cutoff for the data set. M_o is seismic moment, $E^{0.5}$ is Benioff strain energy release, and N is event count. Dashed lines indicate no stable solution or a solution within the range of the data used.

DATA Mmin	Time Period	M_o m	M_o n	M_o α	M_o t_f	$E^{0.5}$ m	$E^{0.5}$ n	$E^{0.5}$ α	$E^{0.5}$ t_f	$E^{0.5}$ Mag	N m	N n	N α	N t_f	NOTE
N,C,S 5.0	1927.1-1988.5	-.945	1.95	1.51	1996.0	.348	.652	2.53	1990.0	6.83	---	---	---	---	m,t_f free
N,C,S 5.0	1927.1-1989.6	-1.52	2.52	1.40	2002.2	.266	.734	2.36	1991.5	7.22	---	---	---	---	m,t_f free
N,C,S 5.0	1939.5-1989.6	-2.00	3.00	1.33	2006.1	.393	.607	2.65	1990.4	6.65	---	---	---	---	m,t_f free
N,C,S 5.0	1964-1989.6	---	---	---	---	---	---	---	---	---	0.537	0.463	3.18	1990.2	m,t_f free
S 5.0	1927.1-1989.6	-1.60	2.60	1.38	2000.4	.355	.645	2.55	1989.9	6.27	---	---	---	---	m,t_f free
N,C,S 5.2	1927.1-1989.6	-2.05	3.05	1.33	2006.1	.126	.874	2.14	1991.7	7.73	---	---	---	---	m,t_f free
N,C,S 5.5	1856.1-1903.6	---	---	---	---	-1.47	2.47	1.40	1938.9	---	.142	.858	2.16	1912.8	m,t_f free
N,C,S 5.5	1856.1-1866.5	-.828	1.83	1.55	1867.3	.101	.899	2.11	1866.6	7.15	---	---	---	---	m,t_f free
N,C,S 5.5	1870.1-1903.6	---	---	---	---	---	---	---	---	---	---	---	---	---	m,t_f free
N,C,S 5.5	1856.1-1903.6	---	---	---	---	.348	.652	2.53	1906.2	7.64	---	---	---	---	fixed m [1]
N,C,S 5.5	1856.1-1903.6	.245	.755	2.32	1906.3	.338	.662	2.51	1906.3	7.69	.439	.561	2.78	1906.3	fixed tf [2]
N,C,S 5.5	1870.1-1903.6	.310	.690	2.45	1906.3	.362	.638	2.57	1906.3	7.63	.444	.556	2.80	1906.3	fixed tf [2]
N,C,S 5.0	1927.1-1989.6	.277	.723	2.38	1989.8	.350	.650	2.54	1990.6	6.81	.442	.558	2.79	2005.0	fixed m [3]
S 5.0	1927.1-1989.6	.277	.723	2.38	1989.8	.350	.650	2.54	1989.9	6.30	.442	.558	2.79	2040.5	fixed m [3]
C 5.0	1955.8-1980.1	.277	.723	2.38	1985.3	.350	.650	2.54	1985.8	6.34	.442	.558	2.79	1985.6	fixed m [3]
N,C,S 5.5	1910.2-1988.5	-.551	1.55	1.65	1992.0	-.571	1.57	1.64	1993.0	---	-.560	1.56	1.64	1994.3	fixed to [4]
N,C,S 5.0	1927.1-1989.6	-.471	1.47	1.68	1993.7	.265	.735	2.36	1991.5	7.23	1.00	0.00	---	---	b1.02
		-.220	1.22	1.82	1992.0	.391	.609	2.64	1990.2	6.59	1.00	0.00	---	---	b1.23
		-.042	1.04	1.96	1991.0	.479	.521	2.92	1989.7	5.99	1.00	0.00	---	---	b1.44
S 5.0	1927.1-1989.6	-.531	1.53	1.65	1993.3	.235	.765	2.31	1990.5	6.94	1.00	0.00	---	---	b0.98
		-.220	1.22	1.82	1991.6	.391	.609	2.64	1989.8	6.01	1.00	0.00	---	---	b1.23
		-.014	1.01	1.99	1990.7	.493	.507	2.97	---	---	1.00	0.00	---	---	b1.48

[1] Exponent m fixed to value determined in row 1 (also see Figure 3) for Loma Prieta earthquake.

2 Time of 1906 earthquake held fixed in analysis of pre-1906 data to determine value of exponent m to be applied to pre- Loma Prieta data.

3 Exponent m fixed to value determined from 2 for foreshocks to previous large event in region (1906 earthquake).

4 All data since previous large event (1906.3) used to determine m and t_f for Loma Prieta earthquake. Decelerating and accelerating sequences are superposed. See Figure 5.

LIST of FIGURES

Figure 1. Northern California earthquakes (magnitude 5 and larger) during the periods (a) 1836-1906 and (b) 1906-1990. Subzones of the region examined in this study are indicated by N, C, and S. The location of 1989 Loma Prieta earthquake is marked by the "+" symbol in (b). The region between the arcs in (b) is the intersection of the two regions where magnitude 7+ earthquakes had been anticipated by Keilis-Borok and Kossobokov (1986).

Figure 2. Cumulative plots of (a) seismic moment in Nm, (b) square root of energy in $(Nm)^{0.5}$, and (c) number of events, for the period 1855-1989 for combined zones N, C, and S. The dominant (M_S 8.2) San Francisco earthquake of 1906 has been removed from plots (a) and (b) to better show the patterns preceding the San Francisco and Loma Prieta earthquakes.

Figure 3. Cumulative plots of pre-step values of earthquake parameters (EQP's) seismic moment (a), and square root of energy (b) for northern California earthquakes of magnitude 5 or greater from 1927-1988. The lines are best fit solutions for m and t_f in equation (2). No fit was obtained for the cumulative event count data of Figure 2(c).

Figure 4. Contour plot of rms error/range as a function of time of failure, t_f, and exponent m for the data of Figure 3(b). Our computed best fit t_f and m from the analysis shown in Figure 3(b), tabulated in the top row of Table 1, are indicated by the large dot. The smaller dot is Varnes' original (1988) estimate. Contour interval is 0.0013.

Figure 5. Cumulative plot of seismic moment for earthquakes of magnitude 5.5 and larger in the union of zones N, C, and S for the time between the 1906 San Francisco and 1989 Loma Prieta earthquakes. The data are fit by superposition of decelerating (aftershock) and accelerating (foreshock) sequences.

Figure 6. Contour plot of rms error/range as a function of magnitude coefficient c and exponent m for the data of Figure 3, with t_f fixed at the time of the Loma Prieta earthquake (1989.8). Contour interval is 0.001. The dashed line shows the relation between m and c from equation (7), for b=1.22, the value computed for the events used in Figure 3.

Figure 7. Simulated evolution of a Loma Prieta earthquake forecast. As events are added to the data set, computed main shock magnitude (top, Fig. 7a) and time of failure (bottom, Fig. 7b) are displayed as functions of time of the last event in the data set. Data used are shown as +'s in Figure 2(b), beginning with the 1927 earthquake. Exponent m is fixed at 0.35 based on analysis of buildup of Benioff strain-energy release preceding the 1906 earthquake (see Table 1). Horizontal dashed lines correspond to the actual time and magnitude (M_L) of the Loma Prieta earthquake. The dotted diagonal line represents points of equal time on the axes of Figure 7b.

Figure 8. Simulated evolution of a 1906 San Francisco earthquake forecast. As events are added to the data set, computed main shock magnitude (top, Fig. 8a) and time of failure (bottom, Fig. 8b) are displayed as functions of time of the last event in the data set. Data used are shown as +'s in Figure 2(b), beginning with the first earthquake in 1855 and ending with the last pre-1906 event in 1903. Dashed horizontal lines correspond to the actual times and magnitudes of the 1836, 1838, 1868, and 1906 earthquakes. The dotted diagonal line represents points of equal time on the axes of Figure 8b.

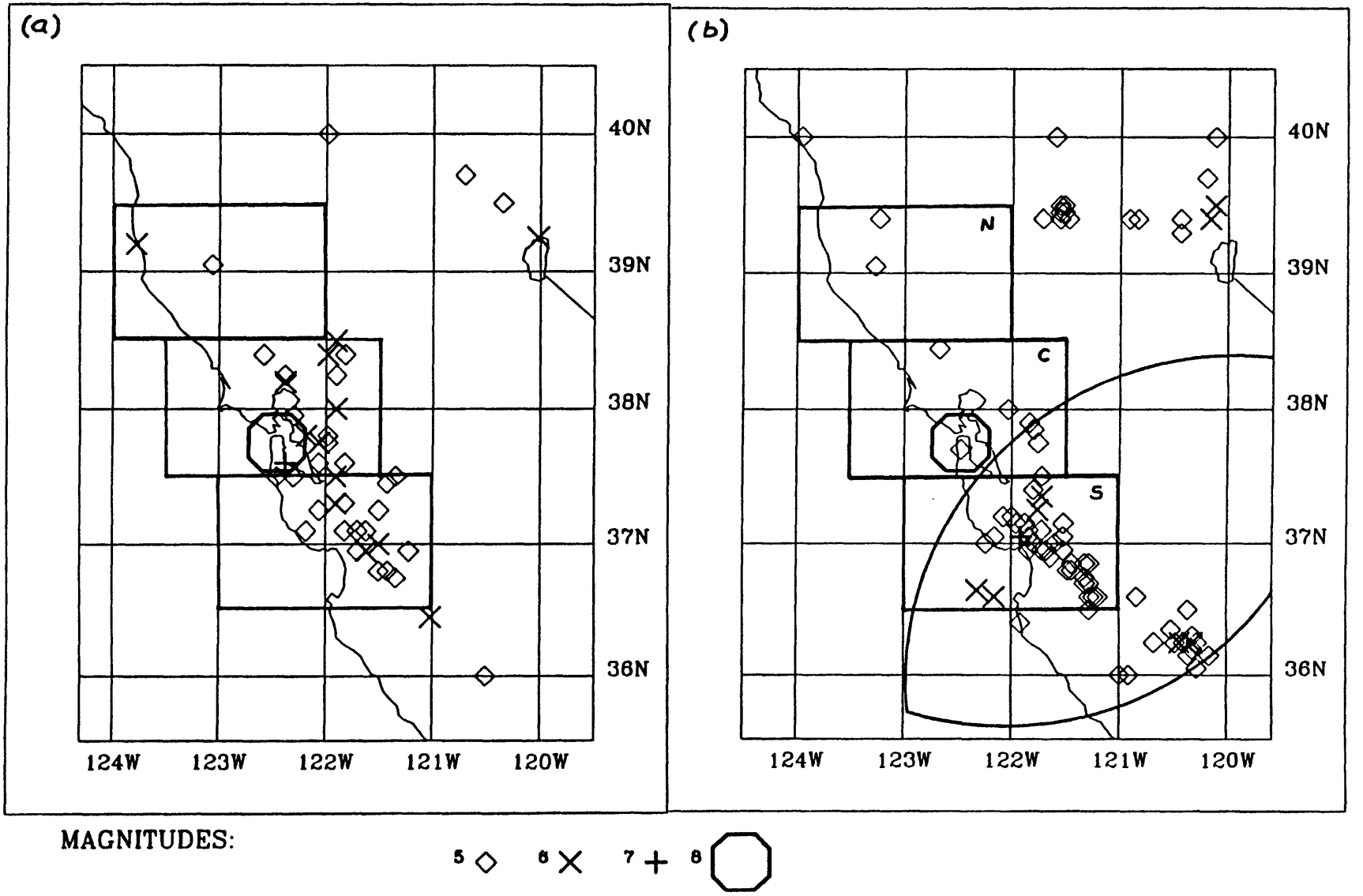

Figure 1. Northern California earthquakes (magnitude 5 and larger) during the periods (a) 1836-1906 and (b) 1906-1990. Subzones of the region examined in this study are indicated by N, C, and S. The location of 1989 Loma Prieta earthquake is marked by the "+" symbol in (b). The region between the arcs in (b) is the intersection of the two regions where magnitude 7+ earthquakes had been anticipated by Keilis-Borok and Kossobokov (1986).

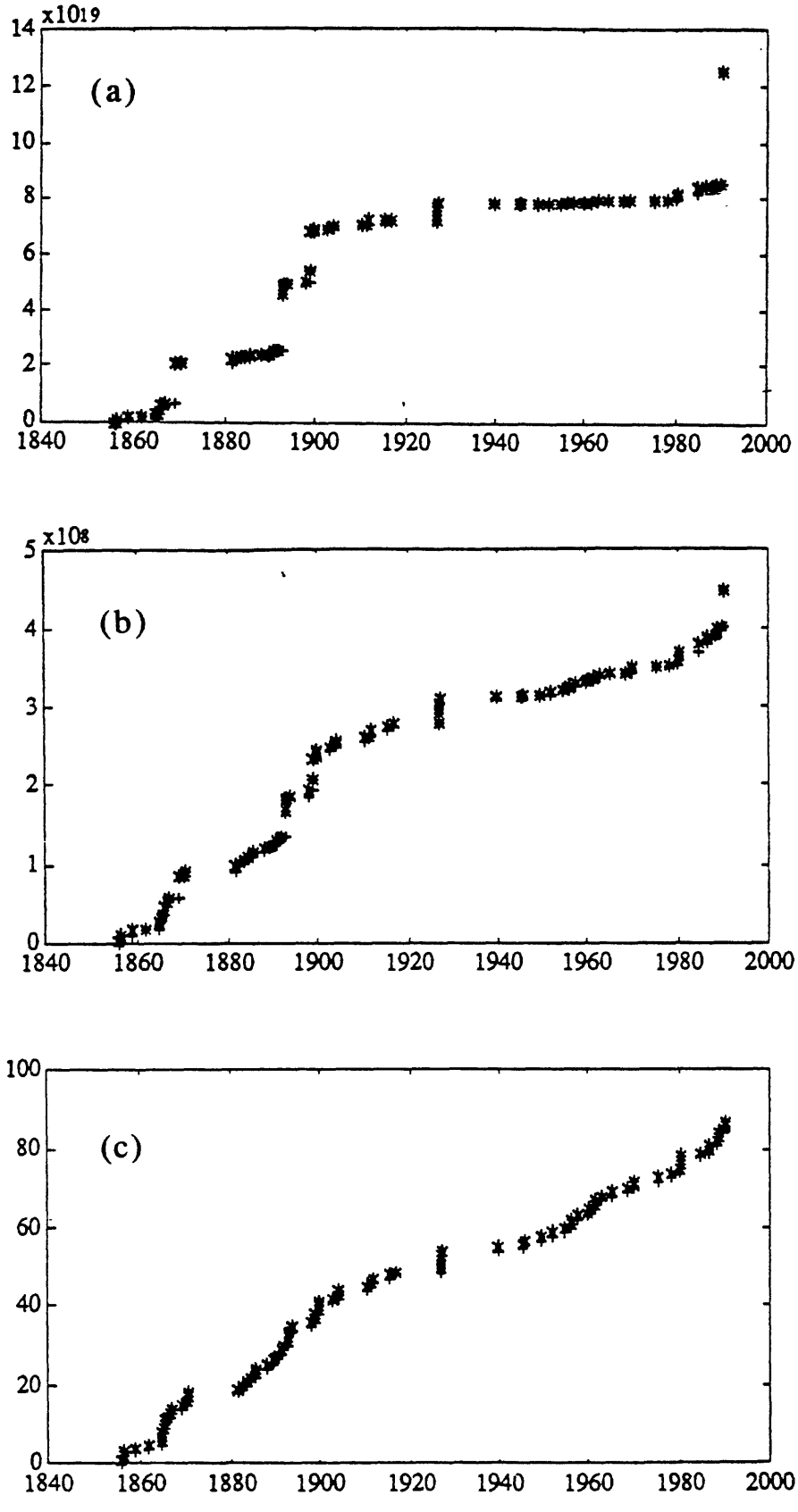

Figure 2. Cumulative plots of (a) seismic moment in Nm, (b) square root of energy in $(Nm)^{0.5}$, and (c) number of events for the period 1855-1989 for combined zones N, C, and S. The dominant (M_s 8.2) San Francisco earthquake of 1906 has been removed from plots (a) and (b) to better show the patterns preceding the San Francisco and Loma Prieta earthquakes.

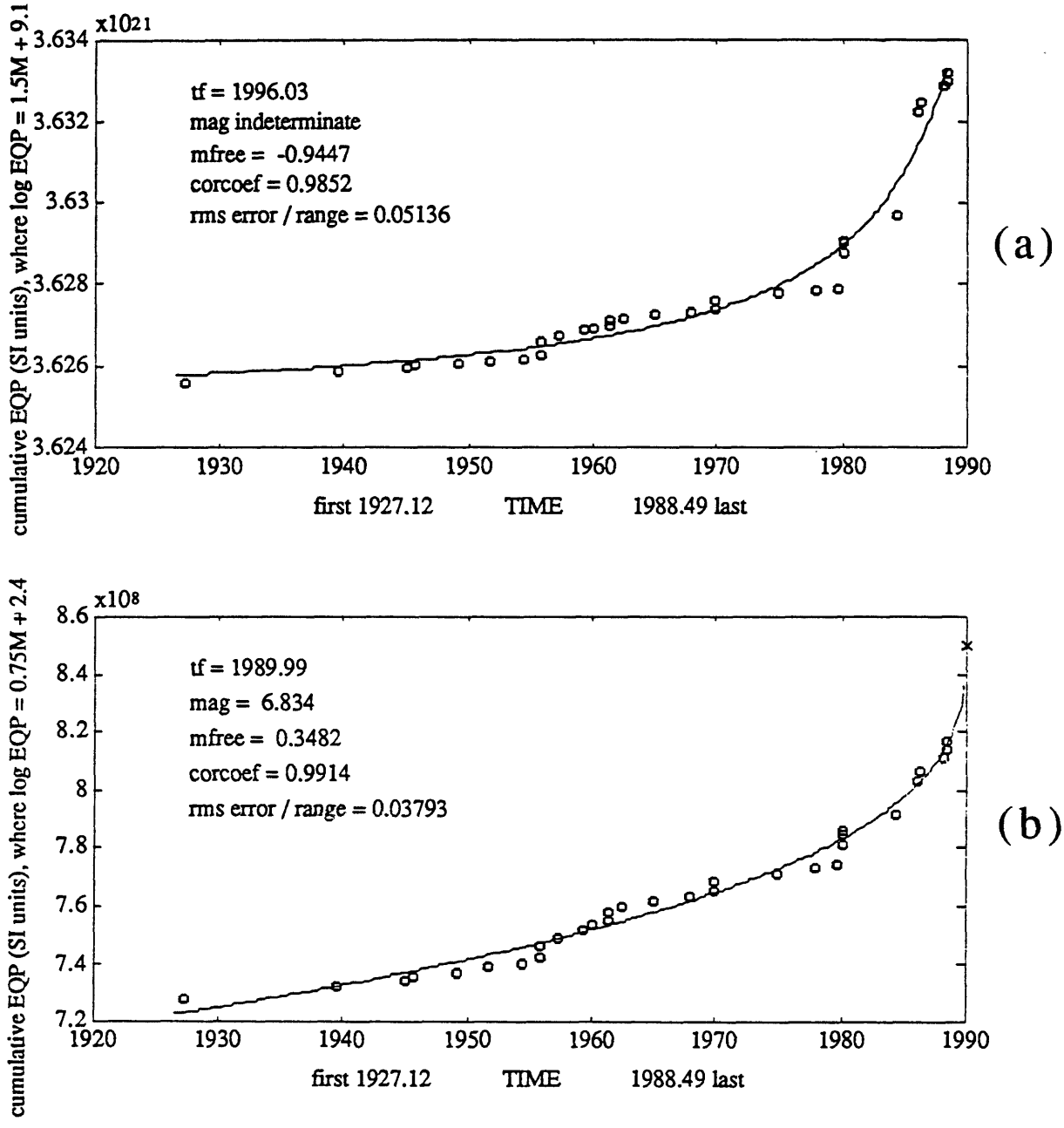

Figure 3. Cumulative plots of pre-step values of earthquake parameters (EPQ's) seismic moment (a), and square root of energy (b) for northern California earthquakes of magnitude 5 or greater from 1927-1988. The lines are best fit solutions for m and tf in equation (2). No fit was obtained for the cumulative event count data of Figure 2(c).

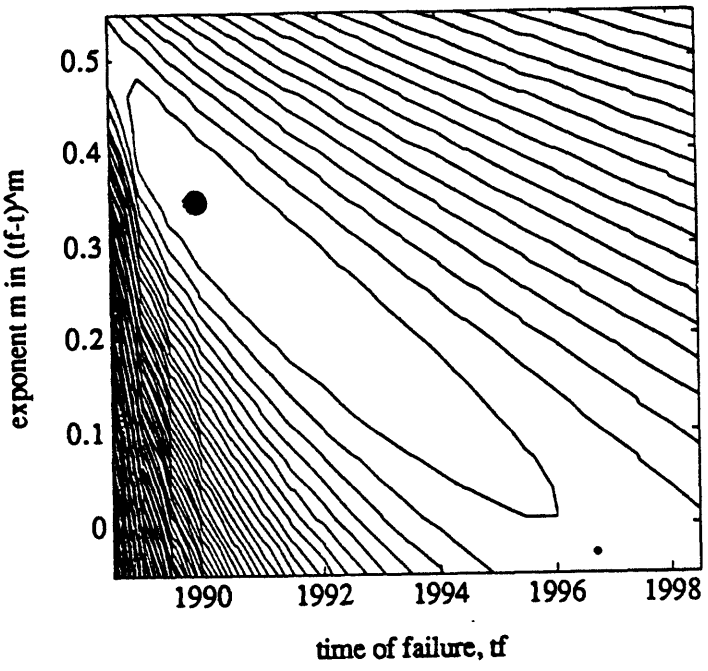

Figure 4. Contour plot of rms error/range as a function of time of failure, t_f, and exponent m for the data of Figure 3(b). Our computed best fit t_f and m from the analysis shown in Figure 3(b), tabulated in the top row of Table 1, are indicated by the large dot. The smaller dot is Varnes original (1988) estimate. Contour interval is 0.0013.

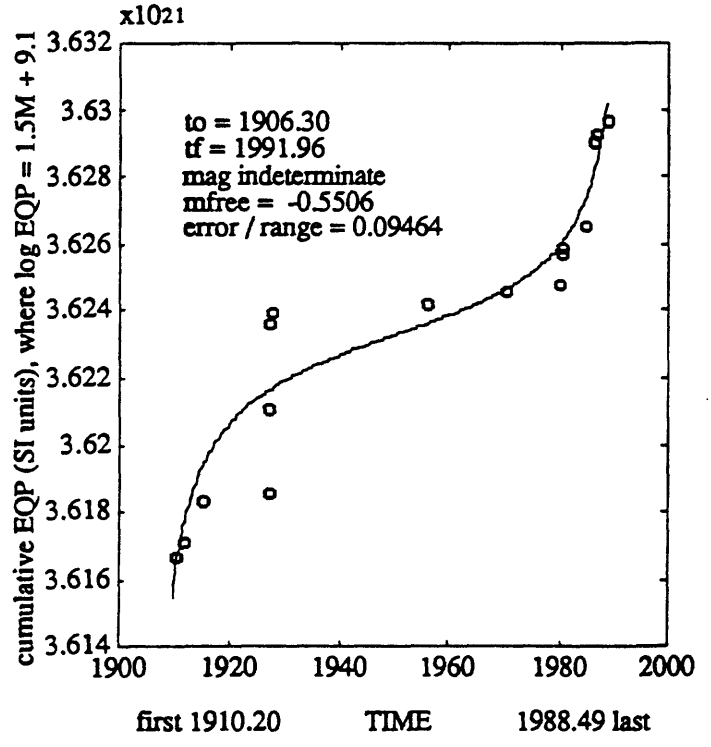

Figure 5. Cumulative plot of seismic moment for earthquakes of magnitude 5.5 and larger in the union of zones N, C, and S for the time between the 1906 San Francisco and 1989 Loma Prieta earthquakes. The data are fit by superposition of decelerating (aftershock) and accelerating (foreshock) sequences.

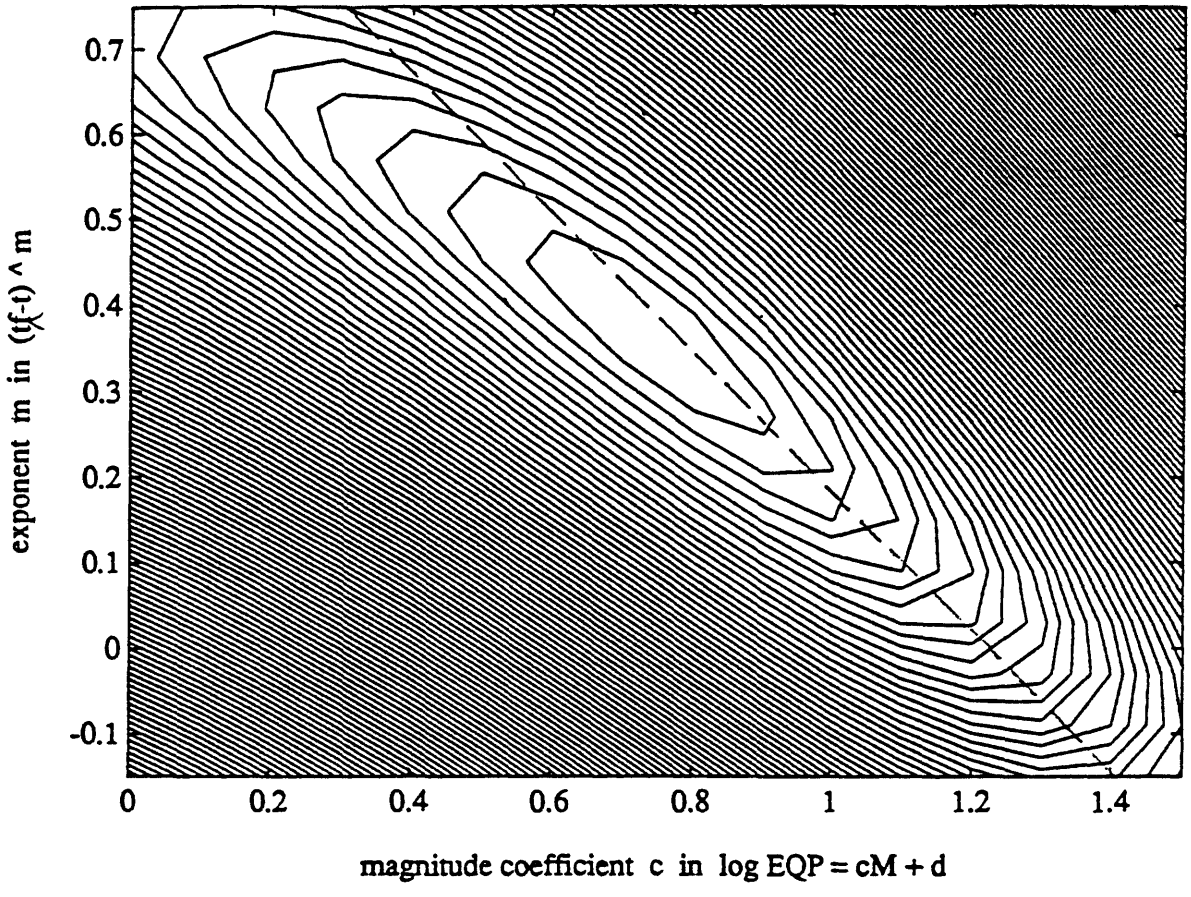

Figure 6. Contour plot of rms error/range as a function of magnitude coefficient c and exponent m for the data of Figure 3, with tf fixed at the time of the Loma Prieta earthquake (1989.8). Contour interval is 0.001. The dashed line shows the relation between m and c from equation (7), for b=1.22, the value computed for the events used in Figure 3.

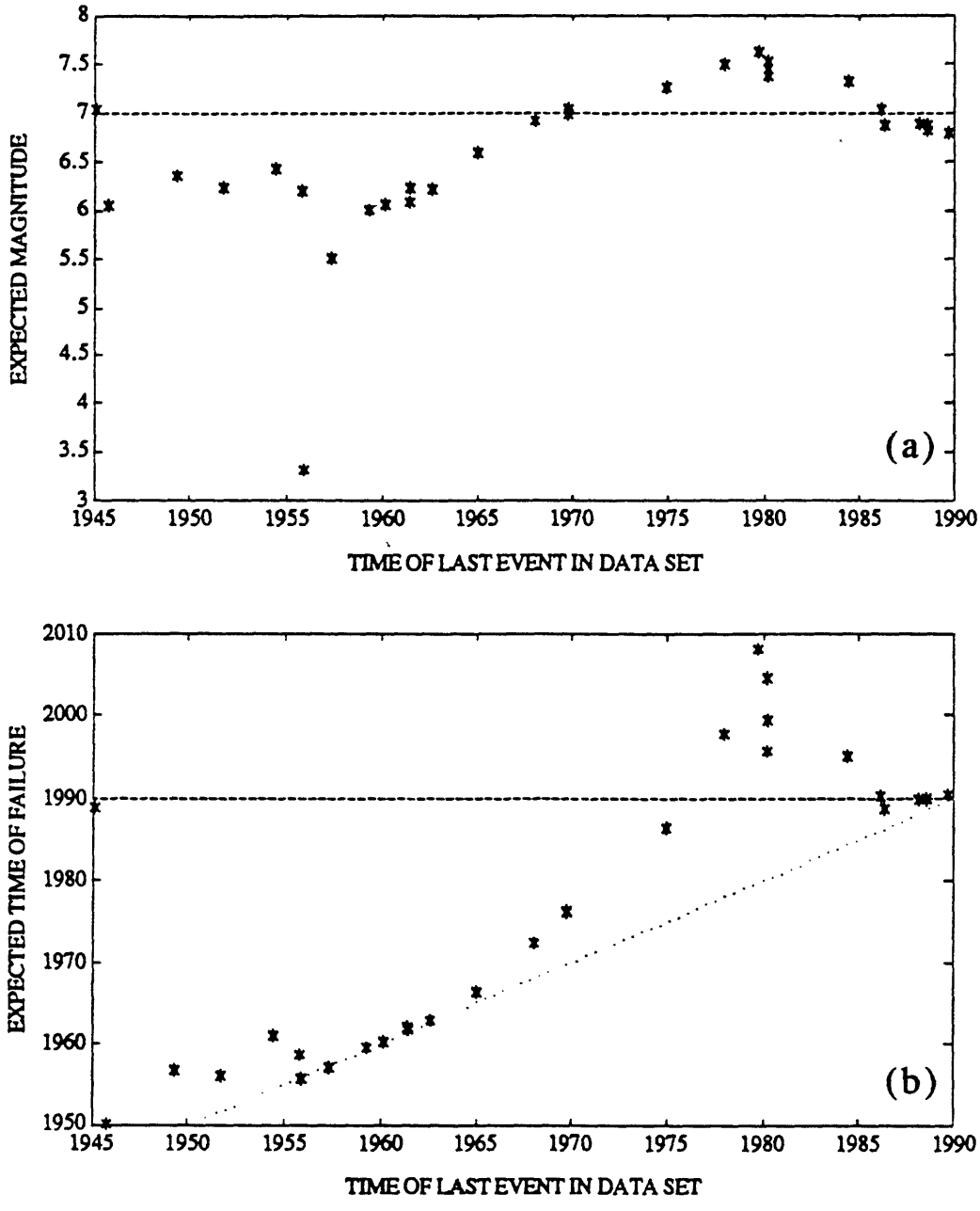

Figure 7. Simulated evolution of a Loma Prieta earthquake forecast. As events are added to the data set, computed main shock magnitude (top, Fig. 7a) and time of failure (bottom, Fig. 7b) are displayed as functions of time of the last event in the data set. Data used are shown as +'s in Figure 2(b), beginning with the 1927 earthquake. Exponent m is fixed at 0.35 based on analysis of buildup of Benioff strain energy release preceding the 1906 earthquake (see Table 1). Horizontal dashed lines correspond to the actual time and magnitude (ML) of the Loma Prieta earthquake. The dotted diagonal line represents points of equal time on the axes of Figure 7b.

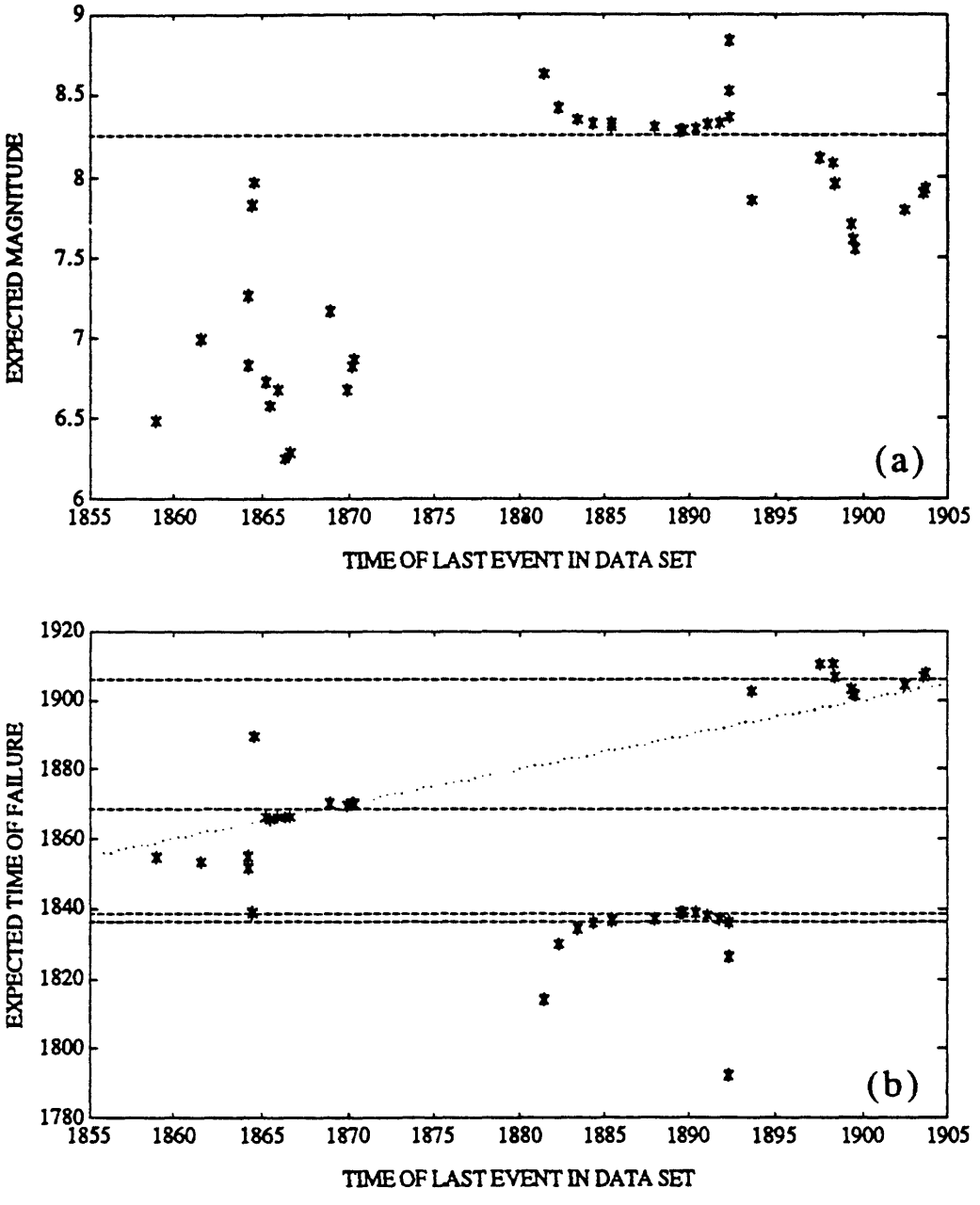

Figure 8. Simulated evolution of a 1906 San Francisco earthquake forecast. As events are added to the data set, computed main shock magnitude (top, Fig. 8a) and time of failure (bottom, Fig. 8b) are displayed as functions of time of the last event in the data set. Data used are shown as +'s in Figure 2(b), beginning with the first earthquake in 1855 and ending with the last pre-1906 event in 1903. Dashed horizontal lines correspond to the actual times and magnitudes of the 1836, 1838, 1868, and 1906 earthquakes. The dotted diagonal line represents points of equal time on the axes of Figure 8b.